

Kinetics and Thermodynamics of Reactions Involving Criegee Intermediates: An Assessment of Density Functional Theory and Ab Initio Methods Through Comparison with CCSDT(Q)/CBS Data

Cameron D. Smith, and Amir Karton *

Reactions involving Criegee intermediates (Cl_s, R₁R₂COO) are important in atmospheric ozonolysis models. In recent years, density functional theory (DFT) and CCSD(T)-based ab initio methods are increasingly being used for modeling reaction profiles involving Cl_s. We obtain highly accurate CCSDT(Q)/CBS reaction energies and barrier heights for ring-closing reactions involving atmospherically important Cl_s (R₁/R₂ = H, Me, OH, OMe, F, CN, cyclopropene, ethylene, acetaldehyde, and acrolein). We use this benchmark data to evaluate the performance of DFT, double-hybrid DFT (DHDFT), and ab initio methods for the kinetics and thermodynamics of these reactions. We find that reaction energies are more challenging for approximate theoretical procedures than barrier heights. Overall, taking both reaction energies and barrier heights into account, only one of the 58 considered DFT methods (the meta-GGA MN12-L) attains near chemical accuracy, with root-mean-square

deviations (RMSDs) of 3.5 (barrier heights) and 4.7 (reaction energies) kJ mol⁻¹. Therefore, MN12-L is recommended for investigations where CCSD(T)-based methods are not computationally feasible. For reaction barrier heights performance does not strictly follow Jacob's Ladder, for example, DHDFT methods do not perform better than conventional DFT methods. Of the ab initio methods, the cost-effective CCSD(T)/CBS(MP2) approach gives the best performance for both reaction energies and barrier heights, with RMSDs of 1.7 and 1.4 kJ mol⁻¹, respectively. All the considered Gaussian-*n* methods show good performance with RMSDs below the threshold of chemical accuracy for both reaction energies and barrier heights, where G4(MP2) shows the best overall performance with RMSDs of 2.9 and 1.5 kJ mol⁻¹, respectively. © 2019 Wiley Periodicals, Inc.

DOI: 10.1002/jcc.26106

Introduction

Criegee intermediates (Cl_s) are important intermediates in the ozonolysis of unsaturated hydrocarbons in the atmosphere, with the reaction mechanism first proposed by Rudolf Criegee.^[1] Since Cl_s are highly reactive and are difficult to study experimentally, quantum chemistry plays a key role in providing mechanistic insights and shaping our current understanding of their chemical reactivity.^[2–4] While reaction mechanisms involving very small Cl_s can be studied using post-CCSD(T) coupled-cluster methods (normally up to CCSDT(Q))^[5–10] most high-level ab initio studies are carried out using the computationally more economical CCSD(T) method.^[11–28] However, for computational studies exploring reaction mechanisms involving larger Cl_s density functional theory (DFT) provides the only practical avenue, and a number of such investigations have been reported in recent years.^[11,14,29–43]

It is therefore of interest to assess the performance of ab initio and DFT methods for their ability to accurately calculate the reaction energies and barrier heights of chemical reactions involving Cl_s. In the present work, we introduce a representative benchmark database of 22 ring-closing reactions involving Cl_s (also known as the Criegee22 database). We calculate the reaction energies and barrier heights of these reactions at the CCSDT(Q)/CBS level of theory by means of the W3lite-F12

composite procedure.^[44–46] These benchmark values allow us to assess the performance of a wide range of standard and composite CCSD(T) methods, MP2-based methods, and contemporary DFT and double-hybrid DFT methods across the rungs of Jacob's Ladder.^[47]

Computational Methods

We use the high-level W3lite-F12 composite procedure for obtaining reaction energies and barrier heights at the CCSDT(Q)/CBS level (i.e., coupled cluster with single, double, triple, and quasiperturbative quadruple excitations at the complete basis set limit). The computational protocol of W3lite-F12 theory has been specified and rationalized elsewhere.^[44–46] The steps involved in W3lite-F12 theory are summarized in Table 1. In this context, it is worth mentioning that for the largest system considered in the present work consisting of seven

C. D. Smith, A. Karton

School of Molecular Sciences, The University of Western Australia, Perth, Western Australia, 6009, Australia

E-mail: amir.karton@uwa.edu.au

Australian Research Council (ARC) Future Fellowship (Project No. FT170100373).

Contract Grant sponsor: Australian Research Council; Contract Grant number: FT170100373

© 2019 Wiley Periodicals, Inc.

Table 1. Steps involved in the high-level W3lite-F12 composite method used for obtaining relativistic, all-electron CCSDT(Q)/CBS reference reaction energies and barrier heights.

Step	Level of theory	Taken from
Hartree–Fock	HF*/VQZ-F12 ^[a]	W2-F12 theory ^[44]
CCSD	V{T,Q}Z-F12	W2-F12 theory ^[44]
(T)	VTZ-F12	W2-F12 theory ^[44]
T–(T)	V{D,T(1d)}Z-F12 ^[b]	W2-F12 theory ^[44]
(Q)	VDZ	W3lite theory ^[45]
Core-valence	CCSD(T)/CBS ^[c]	W2-F12 theory ^[44]
Scalar relativistic	CCSD(T)/A'VTZ-DK ^[d]	W2-F12 theory ^[44]

[a] HF* indicates that the complementary auxiliary basis set (CABS) singles correction is included.^[48–51]
[b] The VTZ(1d) basis set is a truncated version of the VTZ basis set in which the sp functions from the VTZ basis set are combined with the d functions from the VDZ basis set.
[c] The CCSD inner-shell contribution is calculated with the aug-cc-pwCVTZ basis set^[52] and the (T) inner-shell contribution is calculated with the cc-pwCVTZ basis set without the f functions.
[d] Taken as the difference between nonrelativistic CCSD(T)/A'VTZ and relativistic CCSD(T)/A'VTZ-DK calculations (A'VTZ indicates the combination of the regular correlation consistent basis set on hydrogen and aug-cc-pVnZ on first-row elements).

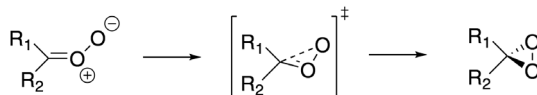


Figure 1. Schematic representation of the reactions in the Criegee22 database. The R₁ and R₂ functional groups are shown in Figure 2.

nonhydrogen atoms (11, Fig. 2) the computational cost of the high-level coupled-cluster calculations involved in W3lite-F12 theory proved to be almost prohibitive with the computational resources at hand. For example, the iterative CCSDT/cc-pVTZ (1d) calculation involves 6.7 billion amplitudes. This calculation required 22 iterations to converge to 10⁻⁶ Hartree. Each iteration ran for about 17 h on 20 cores of a dual Intel Xeon machine (E5-2683-v3 and 2.0 GHz) with 512 GB of RAM, with a total runtime of 16 days. In contrast, a DFT single point energy calculation for the same system requires only a few minutes to complete on four cores and 32 GB of RAM.

Prior to running the W3lite-F12 single-point energy calculations, we performed a preliminary benchmark study of the equilibrium and transition structures obtained by a number of DFT methods. Reference structures for the reactants, transition structures, and products involved in reactions 1, 3-cis, 3-trans, 4-cis, and 4-trans were optimized at the CCSD(T)-F12/cc-pVDZ-F12 level of theory. We note that this level of theory has been found to give geometries that are in good agreement with CCSD(T)/cc-pV6Z geometries for a wide and diverse set of small molecules.^[53] We considered the B3LYP-D3BJ, M06-2X, MN15, and DSD-PBEP86-D3BJ functionals in conjunction with the Def2-TZVPP basis set.^[54] Over the entire set of bond distances, we obtain the following root-mean-square deviations (RMSDs): 0.009 (B3LYP-D3BJ), 0.019 (M06-2X), 0.018 (MN15), and 0.009 (DSD-PBEP86-D3BJ) Å (for further details see Table S1, Supporting Information). These results indicate that the B3LYP-D3BJ and DSD-PBEP86-D3BJ functionals show similar performance. Nevertheless, we opted on using the DSD-PBEP86-D3BJ

Table 2. DFT exchange-correlation functionals considered in the present work. These methods are benchmarked in conjunction with the Def2-QZVPP basis set.

Type ^[a]	Functionals
GGA	BLYP, ^[63,64] B97-D, ^[65] HCTH407, ^[66] PBE, ^[67] BP86, ^[63,68] BPW91, ^[64,69] SOGGA11, ^[70] N12 ^[71] M06-L, ^[72] TPSS, ^[73] τ-HCTH, ^[74] VSXC, ^[75] BB95, ^[76] M11-L, ^[77] MN12-L, ^[78] MN15-L ^[79] BH&HLYP, ^[80] B3LYP, ^[63,81,82] B3P86, ^[68,81] B3PW91, ^[69,81] PBE0, ^[83] B97-1, ^[84] B98, ^[85] X3LYP, ^[86] SOGGA11-X, ^[87] APF, ^[88] APF-D, ^[88] mPW1PW91, ^[69,89] mPW1LYP, ^[63,89] mPW1PBE, ^[67,89] mPW3PBE, ^[67,89] HSE03, ^[90] HSE06 ^[91]
HMGGA	M05, ^[92] M05-2X, ^[93] M06, ^[94] M06-2X, ^[94] M06-HF, ^[94] M08-HX, ^[95] MN15, ^[79] BMK, ^[96] B1B95, ^[63,76] TPSSH, ^[97] τ-HCTH, ^[74] PW6B95 ^[98] ωB97, ^[99] ωB97X, ^[99] ωB97X-D, ^[100] M11, ^[101] N12-SX, ^[102] MN12-SX, ^[102] CAM-B3LYP, ^[103] LC-ωHPBE, ^[104] LC-ωPBE, ^[105] LC-BLYP, ^[106] LC-PBE, LC-BP86, and LC-BPW91 ^[106]
RS	B2-PLYP, ^[107] mPW2-PLYP, ^[108] PBE0-DH, ^[109] PBEQ1-DH, ^[110] B2GP-PLYP, ^[111] B2K-PLYP, ^[112] B2T-PLYP, ^[112] DSD-BLYP, ^[113] DSD-PBEP86 ^[56,57]
DH	

[a] DH, double hybrid; GGA, generalized gradient approximation; HMGGA, hybrid-GGA; MGGGA, hybrid-meta-GGA; RS, range separated.

functional, which should in principle be more reliable since the underlying exchange-correlation functional includes both exact Hartree–Fock exchange and MP2 correlation energies.^[55–58] Finally, we note that in order to enable a rigorous comparison between the benchmark W3lite-F12 and the DFT results, all the DFT calculations are carried out on the DSD-PBEP86-D3BJ/Def2-TZVPP optimized geometries that were used in the W3lite-F12 calculations.

The DFT exchange-correlation functionals considered in the present study (ordered by their rung on Jacob's Ladder)^[47] are given in Table 2. Empirical D3 dispersion corrections^[59–61] are included in some cases using the finite Becke–Johnson^[62] and zero-damping potentials (denoted by the suffix -D3BJ and -D3, respectively). We note that the suffix -D in B97-D and ωB97X-D indicates the original dispersion correction. In the following discussion we will regard to DFT methods with RMSDs from our CCSDT(Q)/CBS reference values smaller than ~4 kJ mol⁻¹ as good performers and to methods with RMSDs that are twice as large (i.e., RMSD > ~8 kJ mol⁻¹) as poor performers.

The performance of CCSD(T) and MP2-based ab initio methods is also assessed. We consider the performance of the following standard ab initio methods: MP2, SCS-MP2,^[114] SOS-MP2,^[115] SCS(MI)-MP2,^[116] SCSN-MP2,^[117] S2-MP2,^[118] and CCSD(T).^[119,120] In addition, we consider the following composite procedures: G4,^[121] G4(MP2),^[122] G4(MP2)-6X,^[123] G3B3,^[124] G3(MP2)B3,^[124] and CBS-QB3.^[125] All the DFT, DHDF, and MP2 calculations were carried out in conjunction with the Def2-QZVPP basis set.^[54] All the CCSD(T) calculations involved in the W3lite-F12 protocol were calculated using Molpro 2016,^[126,127] while all post-CCSD(T) calculations were performed using the MRCC program.^[128,129] All the other calculations

(DFT, DHDFT, MP2, and lower-level composite procedures) were performed using the Gaussian 16 program suite.^[130]

Results and Discussion

Overview of the reactions and benchmark CCSDT(Q)/CBS reaction energies and barrier heights in the Criegee22 database

The Criegee22 database is comprised of 22 reaction energies and barrier heights for the ring-closing reaction shown in Figure 1. The 22 reactants are shown in Figure 2. In all of these reactions the terminal oxygen of the Cl reactant attacks the carbonyl carbon to form a dioxirane ring.

Table 3 lists the CCSDT(Q)/CBS reaction energies (ΔE_r) and barrier heights (ΔE^\ddagger) for the reactions in the Criegee22 database. To ensure we are comparing apples to apples, so to speak, relativistic effects are included when benchmarking composite ab initio methods but are excluded when benchmarking DFT, DHDFT, and standard ab initio methods. However, we note that the difference between the relativistic and nonrelativistic reaction energies and barrier heights is fairly small and ranges between 0.1 and 0.4 kJ mol⁻¹ (see Table S2).

A recent study examined a set of CCSDT(Q)/CBS barrier heights for a diverse range of reactions, including pericyclic, bipolar cycloaddition, cycloreversion, and multiple-proton transfer reaction.^[131] They found that CCSD(T)/CBS reaction barrier heights normally benefit from an effective error cancellation between the higher-order triples, T-(T), which tend to increase the barrier heights, and the quasiperturbative quadruples, (Q),

Table 3. CCSDT(Q)/CBS reaction energies (ΔE_r) and barrier heights (ΔE^\ddagger) for the reactions in the Criegee22 database obtained using W3lite-F12 theory (in kJ mol⁻¹).^[a]

	Reaction energies (ΔE_r)		Barrier heights (ΔE^\ddagger)	
	nonrel ^[b]	rel ^[c]	nonrel ^[b]	rel ^[c]
1	-105.2	-105.4	83.0	82.7
2-cis	-92.3	-92.5	103.4	103.1
2-trans	-107.5	-107.8	69.6	69.3
3-cis	-112.6	-112.8	84.1	83.8
3-trans	-117.5	-117.6	30.8	30.6
4-cis	-145.5	-145.7	78.7	78.4
4-trans	-150.2	-150.3	37.5	37.2
5-cis-anti	-106.7	-106.9	80.3	80.1
5-cis-syn	-111.9	-112.1	51.9	51.6
5-trans-anti	-111.4	-111.5	28.2	28.0
5-trans-syn	-111.0	-111.1	31.4	31.2
6	-107.1	-107.2	37.1	36.9
7-cis-anti	-81.4	-81.7	85.9	85.5
7-cis-syn	-70.3	-70.5	113.2	112.9
7-trans-anti	-84.3	-84.6	74.1	73.8
7-trans-syn	-84.2	-84.5	63.0	62.7
8-cis	-86.6	-86.7	104.7	104.4
8-trans	-109.9	-110.1	71.6	71.2
9	-90.4	-90.6	91.5	91.2
10-cis	-94.8	-95.1	92.0	91.6
10-trans	-96.8	-97.1	80.9	80.5
11	-80.7	-81.0	82.2	81.8

[a] For the component breakdown of the W3lite-F12 reaction energies and barrier heights see Table S2 of the Supporting Information.

[b] All-electron, nonrelativistic CCSDT(Q)/CBS reference values from W3lite-F12 theory for benchmarking DFT and standard ab initio procedures.

[c] All-electron, relativistic CCSDT(Q)/CBS reference values from W3lite-F12 theory for benchmarking composite ab initio procedures.

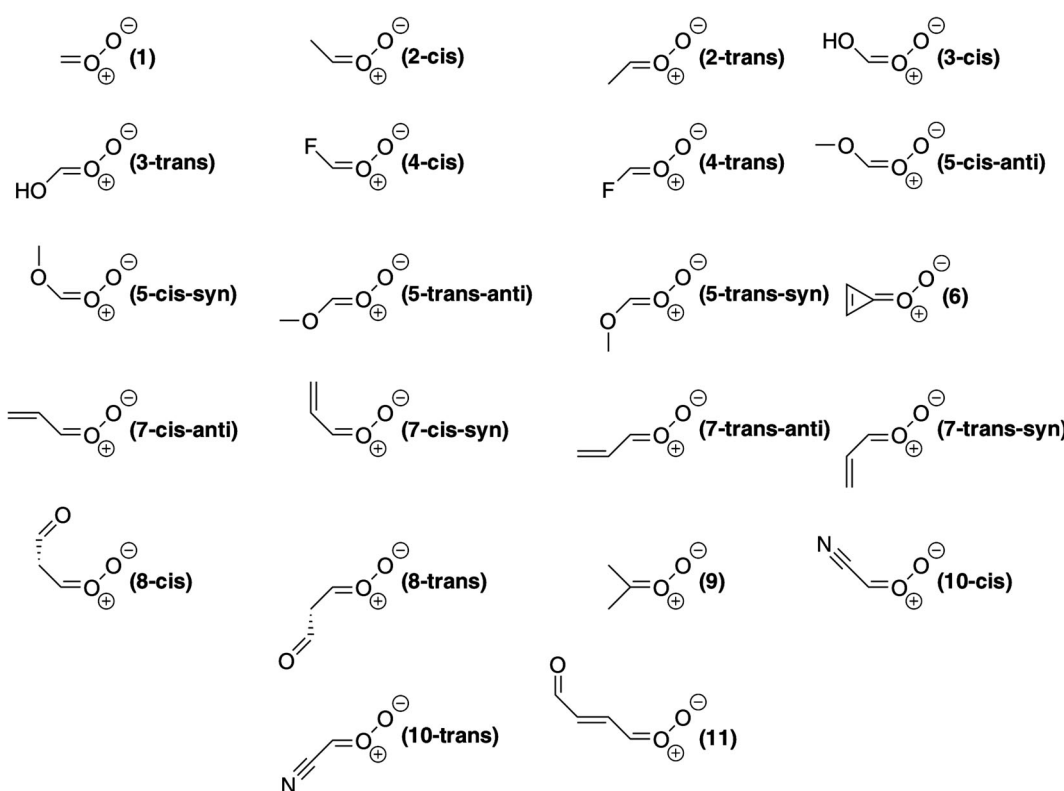


Figure 2. Reactants involved in the Criegee22 database (see Fig. 1 for a schematic representation of the ring-closing reaction).

which tend to reduce the barrier heights. Thus, overall post-CCSD(T) contributions to reaction barrier heights normally do not exceed the 1 kJ mol^{-1} mark. A striking exception to this are the challenging cycloreversion fragmentation reactions for which the T-(T) and (Q) contributions reinforce each other,^[131] and thus post-CCSD(T) contributions can reach up to 6.7 kJ mol^{-1} . Inspection of Table S2 reveals that post-CCSD(T) contributions to the reaction barrier heights in the Criegee22 database do not exceed the 1.5 kJ mol^{-1} mark and are therefore consistent with the general finding of ref. [131]. On the other hand, post-CCSD(T) contributions to the reaction energies in the Criegee22 database are much larger. In particular, in 50% of the cases they exceed 4.0 kJ mol^{-1} , and can reach up to 8.0 kJ mol^{-1} . Thus, it is clear that CCSD(T)/CBS reaction energies (e.g., from W_n or $W_n\text{-F12}$,^[44,132] $n = 1$ and 2) are not sufficiently accurate for benchmarking more approximate quantum chemical procedures.

The relativistic, all-electron, vibrationless CCSDT(Q)/CBS reaction energies in the Criegee22 database (all exothermic) range between 70.5 and $150.3 \text{ kJ mol}^{-1}$, and the barrier heights range between 28.0 and $112.9 \text{ kJ mol}^{-1}$. We note that our reaction barrier height for the cyclization of the prototypical Cl (CH_2OO) of 82.7 kJ mol^{-1} is in good agreement with the recently reported experimental value of 81.8 kJ mol^{-1} fitted via master equation calculations to CH_2OO decomposition kinetics obtained from ultraviolet experiments.^[133]

In cases where the substituent cis to the terminal oxygen (R_1) involves an electronegative atom attached to the carbonyl carbon of the Cl, the barrier height for the ring closing reaction is significantly higher. For example, for $R = \text{OH}$, we obtain the following reaction barrier heights 83.8 (3-cis) and 30.6 (3-trans) kJ mol^{-1} (Table 3). Similarly, for $R = \text{F}$, we obtain reaction barrier heights of 78.4 (4-cis) and 37.2 (4-trans) kJ mol^{-1} .

Performance of DFT and DHDFT procedures for the reaction barrier heights in the Criegee22 database

Figure 3 and Table 4 give an overview of the performance of 58 DFT and 9 DHDFT functionals. Dispersion effects play a minor

role for both reaction energies and barrier heights and will be discussed in the subsection Dispersion Corrections. We start by making a few general observations:

- With no exceptions all of the DFT methods overestimate the CCSDT(Q)/CBS barrier heights as reflected by positive mean-signed deviations (MSDs).
- For nearly all functionals across the rungs of Jacob's Ladder, the largest positive deviations are obtained for the reactions involving the strong electron accepting CN group (10-cis and 10-trans).
- The best performing hybrid-GGA (rung 3.5) and double-hybrid (rung 5) functionals show poorer performance relative to the best performers from the other rungs of Jacob's Ladder. Thus, the performance for reaction barrier heights does not strictly improve along the Jacob Ladder rungs.

Of the eight pure GGAs, BLYP shows exceptionally good performance with an RMSD of 3.0 kJ mol^{-1} . The other GGAs result in RMSDs ranging between 5.2 (BP86) and 13.7 (HCTH407) kJ mol^{-1} . Inclusion of the kinetic energy density improves the performance, such that four MGGA procedures result in RMSDs $\leq 4.0 \text{ kJ mol}^{-1}$; namely, TPSS (2.1), MN12-L (3.5), MN15-L (3.6), and BB95 (4.0 kJ mol^{-1}).

None of the hybrid GGAs result in RMSDs $< 4.0 \text{ kJ mol}^{-1}$. The best HGGA functionals (mPW1LYP, B98, and B97-1) attain RMSDs between 4.6 and 4.9 kJ mol^{-1} , while the worst performers (PBE0, HSE03, and HSE06) result in RMSDs of 8.0 – 8.2 kJ mol^{-1} . Inclusion of the kinetic energy density significantly improves performance. The best performing HMGGA functionals are (RMSDs given in parenthesis): MN15 (2.1) and TPSSh (2.6 kJ mol^{-1}). The next HMGGA PW6B95 lags behind with an RMSD of 4.3 kJ mol^{-1} . Thus, there seems to be little or no correlation between the performance and the percentage of exact Hartree–Fock (HF) exchange in the functional form. For example, MN15, TPSSh, and PW6B95 involve 44%, 10%, and 28% of exact HF exchange. Two HMGGAs (M08-HX and M05) show poor

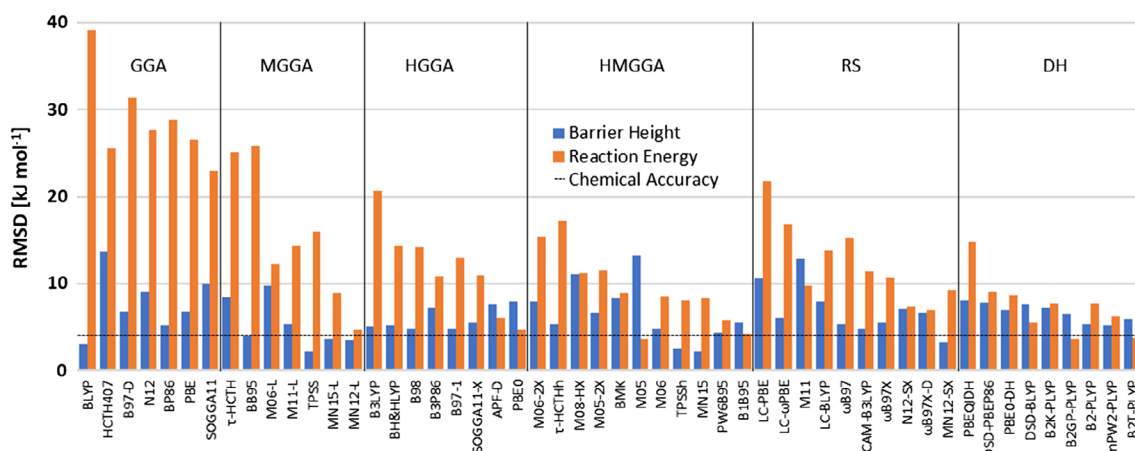


Figure 3. Root-mean-square deviations (RMSDs) of a representative set of DFT and DHDFT procedures over the barrier heights (shown in blue) and reaction energies (shown in orange) for the Criegee22 database (in kJ mol^{-1}). The dashed black line represents an RMSD of 4.2 kJ mol^{-1} , functionals attaining RMSDs below this line are considered good performers. The RMSDs of all the DFT procedures are given in Tables 4 and 5. [Color figure can be viewed at wileyonlinelibrary.com]

Table 4. Statistical analysis for the performance of DFT and DHDFT procedures for the reaction barrier heights in the Criegee22 database (in kJ mol^{-1}). The CCSDT(Q)/CBS reference values are given in Table 3.

Type ^[a]	Method	RMSD ^[b]	MAD ^[b]	MSD ^[b]	LND ^{[b],[c]}	LPD ^{[b],[c]}
GGA	BLYP	3.0	2.6	2.5	-0.8 (8-cis)	5.8 (10-trans)
	BP86	5.2	4.7	4.6	-1.3 (6)	8.0 (10-trans)
	BPW91	5.9	5.4	5.3	-1.2 (6)	8.8 (10-trans)
	B97-D	6.8	6.2	6.2	-0.1 (6)	10.6 (10-trans)
	PBE	6.8	6.2	6.1	-0.8 (6)	9.8 (10-trans)
	N12	9.0	8.6	8.6	N/A	12.9 (10-trans)
	SOGGA11	10.0	8.9	8.9	N/A	15.3 (8-trans)
	HCTH407	13.7	13.1	13.1	N/A	18.0 (10-trans)
	TPSS	2.1	1.8	0.6	-3.5 (6)	4.9 (10-trans)
MGGA	MN12-L	3.5	2.5	2.1	-1.8 (5-cis-anti)	10.0 (10-trans)
	MN15-L	3.6	2.7	2.1	-2.6 (5-cis-syn)	9.8 (10-trans)
	BB95	4.0	3.5	3.2	-2.4 (6)	6.4 (10-trans)
	M11-L	5.2	3.9	3.6	-1.9 (5-cis-syn)	13.6 (10-trans)
	VSXC	6.4	5.6	4.9	-5.5 (5-cis-syn)	12.0 (10-cis)
	τ -HCTH	8.4	7.7	7.7	-0.1 (6)	12.6 (10-trans)
	M06-L	9.7	9.2	9.2	N/A	15.4 (10-trans)
	mPW1LYP	4.6	3.9	3.9	-0.4 (5-cis-anti)	9.6 (10-trans)
	B98	4.8	4.5	4.5	N/A	9.3 (10-trans)
HGGA	B97-1	4.9	4.5	4.5	N/A	9.4 (10-trans)
	B3LYP	5.1	4.7	4.7	N/A	10.0 (10-trans)
	X3LYP	5.2	4.7	4.7	N/A	10.2 (10-trans)
	BH&HLYP	5.2	4.5	2.3	-7.0 (5-cis-anti)	9.3 (10-trans)
	SOGGA11X	5.6	4.9	4.9	N/A	11.4 (10-trans)
	mPW1PW91	7.1	6.8	6.8	N/A	12.8 (10-trans)
	B3P86	7.2	6.9	6.9	N/A	12.4 (10-trans)
	B3PW91	7.3	7.0	7.0	N/A	12.5 (10-trans)
	mPW1PBE	7.3	7.0	7.0	N/A	13.0 (10-trans)
HMGGA	mPW3PBE	7.5	7.2	7.2	N/A	12.7 (10-trans)
	APF-D	7.6	7.2	7.2	N/A	13.1 (10-trans)
	APF	7.7	7.4	7.4	N/A	13.2 (10-trans)
	PBE0	8.0	7.6	7.6	N/A	13.6 (10-trans)
	HSE06	8.1	7.8	7.8	N/A	14.1 (10-trans)
	HSE03	8.2	7.9	7.9	N/A	14.2 (10-trans)
	MN15	2.1	1.7	0.5	-3.5 (5-cis-anti)	5.3 (10-trans)
	TPSSh	2.6	2.1	1.8	-1.4 (6)	7.1 (10-trans)
	PW6B95	4.3	3.9	3.9	N/A	9.7 (10-trans)
RS	M06	4.8	4.4	4.4	N/A	10.4 (10-trans)
	τ -HCTHh	5.3	5.0	5.0	N/A	9.9 (10-trans)
	B1B95	5.5	5.2	5.2	N/A	11.1 (10-trans)
	M06-HF	6.2	4.8	1.3	-10.3 (4-cis)	10.4 (5-trans-anti)
	M05-2X	6.6	6.0	6.0	N/A	12.6 (10-trans)
	M06-2X	8.0	7.5	7.5	N/A	13.4 (10-trans)
	BMK	8.3	8.1	8.1	N/A	12.1 (10-trans)
	M08-HX	11.1	10.5	10.5	N/A	18.6 (10-trans)
	M05	13.3	13.0	13.0	N/A	19.4 (10-trans)
DH	MN12-SX	3.3	2.8	0.4	-5.7 (5-cis-anti)	7.8 (10-trans)
	CAM-B3LYP	4.9	4.3	4.3	N/A	8.9 (10-trans)
	ω B97	5.3	4.7	4.7	N/A	8.4 (10-trans)
	ω B97X	5.6	5.1	5.1	N/A	9.2 (10-trans)
	LC- ω HPBE	6.0	5.8	5.8	N/A	9.0 (10-trans)
	LC- ω PBE	6.0	5.8	5.8	N/A	9.0 (10-trans)
	ω B97X-D	6.7	6.5	6.5	N/A	10.8 (10-trans)
	N12-SX	7.1	6.8	6.8	N/A	12.7 (10-trans)
	LC-BLYP	8.0	7.4	7.4	N/A	12.3 (6)

(Continues)

Table 4. Continued

Type ^[a]	Method	RMSD ^[b]	MAD ^[b]	MSD ^[b]	LND ^{[b],[c]}	LPD ^{[b],[c]}
	DSD-BLYP	7.6	6.6	6.6	N/A	16.4 (10-trans)
	DSD-PBEP86	7.8	6.9	6.9	N/A	16.6 (10-trans)
	PBEQI-DH	8.0	7.4	7.4	N/A	16.2 (10-trans)

[a] Footnote *a* to Table 2 applies here.
[b] LND, largest negative deviation; LPD, largest positive deviation; MAD, mean-absolute deviation; MSD, mean-signed deviation; RMSD, root-mean-square deviation.
[c] The reaction with the LND/LPD is given in parenthesis (see Figs. 1 and 2).

performance with RMSDs of 11.1 and 13.3 kJ mol⁻¹, respectively. Finally, we note that only one of the range-separated functionals (MN12-SX) results in good performance with an RMSD of 3.3 kJ mol⁻¹.

The double-hybrid functionals result in disappointing RMSDs ranging between 5.2 and 8.0 kJ mol⁻¹, where the best performers are the older-generation mPW2-PLYP and B2-PLYP functionals. This result is unexpected since DHDFT functionals have been found to exhibit significant improvement in performance over conventional GGA, MGGA, and HGGA functionals for a wide range of reaction barrier heights.^[134–136] Including hydrogen transfer, heavy atom transfer, nucleophilic substitution, and unimolecular and recombination reactions,^[111,137] uncatalyzed and water-catalyzed proton transfers,^[138] and pericyclic, cycloaddition, and cycloreversion reactions.^[139,140]

Performance of DFT and DHDFT procedures for the reaction energies in the Criegee22 database

Figure 3 and Table 5 give an overview of the performance of the DFT and DHDFT functionals for the reaction energies in the Criegee22 database. Inspection of the results in Table 5 reveals that the reaction energies are much more challenging for conventional DFT methods than the reaction barrier heights. This is seen across rungs 2–4 of Jacob's Ladder, and is demonstrated, for example, by taking the average of the RMSDs for all functionals from each rung. These results are listed in Table 6. The better performance of DFT methods for reaction barrier heights may be attributed to the larger degree of chemical similarity between reactants and TSs rather than with the products which contain a strained dioxirane ring. For the GGA methods the average RMSD goes up from 7.6 for barrier heights up to 28.7 kJ mol⁻¹ for reaction energies. The poor performance of GGAs for the thermochemistry of challenging reactions is not surprising,^[81,134–136,141–144] however, the large difference between the performance for reaction energies and barrier heights highlights the relatively good performance of GGAs for the reaction barrier heights in the Criegee22 database.

For the reaction energies, the RMSDs for the GGAs range from 23.0 (SOGGA11) to 39.1 (BLYP) kJ mol⁻¹ (Table 5). Thus, it is clear that GGAs cannot be used for investigating similar reaction energies. Inclusion of the kinetic energy density significantly improves performance in one case, namely MN12-L attains relatively good performance with an RMSD of 4.7 kJ mol⁻¹. However, the other MGGA show poor performance with RMSDs ranging between 8.9 (MN15-L) and 30.0 (VSXC) kJ mol⁻¹.

Moving on to rung 3.5 of Jacob's Ladder, the HGGA functionals still struggle with the reaction energies in the Criegee22 database, with RMSDs ranging between 4.7 (PBE0) and 20.7 (B3LYP) kJ mol⁻¹. Thus, the best performing MGGA and HGGA (MN12-L and PBE0) result in practically the same RMSD of 4.7 kJ mol⁻¹. Two functionals from rung 4 of Jacob's Ladder (M05 and B1B95) result in good performance with RMSDs of 3.6 and 4.2 kJ mol⁻¹, respectively. However, the rest of the HMGGAs result in RMSDs ranging between 5.8 (PW6B95) and 26.8 (M06-HF) kJ mol⁻¹. Finally, we note that none of the range-separated functionals attain good performance (Table 5).

Two rung 5 functionals, which were optimized for thermochemistry, B2GP-PLYP and B2T-PLYP result in good performance with RMSDs of 3.6 and 3.8 kJ mol⁻¹, respectively. The rest of the double-hybrid functionals result in RMSDs ranging between 5.6 (DSD-BLYP) and 14.7 (PBEQI-DH) kJ mol⁻¹.

Dispersion corrections

Table 7 gathers the differences in RMSD between the dispersion-corrected and uncorrected DFT functionals. We consider both the D3 correction with a zero-damping function and the D3BJ correction with the finite Becke–Johnson damping function. Inspection of the results in Table 7 reveals that, across all rungs of Jacob's Ladder, inclusion of either the D3 or D3BJ correction has a relatively minor effect on the performance of DFT for both the reaction energies and barrier heights in the Criegee22 database. For the reaction barrier heights, the D3 correction leads to no change in the RMSDs or minor deteriorations in performance by up to 0.2 kJ mol⁻¹ (B3LYP, B3PW91, and BMK). The D3BJ correction, on the other hand, leads to minor improvements in performance by up to 0.3 kJ mol⁻¹ (BLYP). For the reaction energies, the D3 correction results in minor changes of up to 0.3 kJ mol⁻¹ (BLYP and BP86) in the RMSDs. The D3BJ correction tends to lead to more significant changes in performance by up to 0.9 kJ mol⁻¹ (BLYP).

Performance of standard and composite ab initio procedures for the reaction energies and barrier heights in the Criegee22 database

Table 8 gives an overview of the performance of standard and composite ab initio methods for the reaction energies and barrier heights in the Criegee22 database. Before proceeding to a detailed discussion of the performance of the MP2 and CCSD(T) methods, we note that it has been recently shown that extrapolating MP2 and CCSD(T) correlation energies using minimal basis can yield correlation energies that outperform those

Table 5. Statistical analysis for the performance of DFT and DHDFT procedures for the reaction energies in the Criegee22 database (in kJ mol⁻¹). The CCSDT(Q)/CBS reference values are given in Table 3.

Type ^[a]	Method	RMSD ^[b]	MAD ^[b]	MSD ^[b]	LND ^{[b],[c]}	LPD ^{[b],[c]}
GGA	SOGGA11	23.0	21.7	21.3	-4.5 (6)	33.9 (10-trans)
	HCTH407	25.5	24.7	24.7	N/A	34.2 (10-trans)
	PBE	26.6	25.9	25.9	N/A	33.0 (10-trans)
	BPW91	27.3	26.8	26.8	N/A	33.2 (10-trans)
	N12	27.6	27.1	27.1	N/A	33.8 (7-trans-anti)
	BP86	28.9	28.4	28.4	N/A	34.4 (11)
	B97-D	31.3	31.0	31.0	N/A	37.7 (10-trans)
MGGA	BLYP	39.1	39.0	39.0	N/A	43.4 (7-trans-anti)
	MN12-L	4.7	4.0	1.3	-12.1 (1)	8.9 (6)
	MN15-L	8.9	8.2	-8.2	-18.5 (1)	N/A
	M06-L	12.3	11.7	11.7	N/A	17.2 (11)
	M11-L	14.3	14.0	14.0	N/A	20.6 (6)
	TPSS	16.0	15.6	15.6	N/A	20.2 (11)
	τ -HCTH	25.1	24.6	24.6	N/A	31.5 (7-trans-syn)
HGGA	BB95	25.9	25.3	25.3	N/A	31.7 (11)
	VSXC	30.0	29.4	29.4	N/A	37.5 (11)
	PBE0	4.7	4.1	3.5	-3.6 (1)	7.8 (3-cis)
	mPW1PBE	5.0	4.4	3.7	-3.8 (1)	7.9 (3-cis)
	mPW1PW91	6.0	5.2	4.7	-3.0 (1)	8.9 (3-cis)
	APF-D	6.1	5.6	5.5	-0.3 (1)	10.1 (3-cis)
	APF	6.9	6.3	6.2	-1.0 (1)	10.2 (3-cis)
HMGGA	HSE03	7.0	6.3	6.2	-1.6 (1)	10.2 (3-cis)
	HSE06	7.0	6.4	6.3	-1.2 (1)	10.3 (3-cis)
	mPW3PBE	9.9	9.5	9.5	N/A	13.1 (3-cis)
	B3PW91	10.5	10.1	10.1	N/A	13.8 (5-cis-anti)
	B3P86	10.9	10.5	10.5	N/A	14.2 (3-cis)
	SOGGA11X	11.0	8.9	-6.7	-21.9 (10-cis)	12.1 (6)
	B97-1	13.0	12.5	12.5	N/A	16.6 (5-cis-anti)
RS	B98	14.2	13.6	13.6	N/A	18.3 (5-trans-syn)
	BH&HLYP	14.3	12.1	0.9	-22.9 (10-cis)	32.8 (6)
	mPW1LYP	18.5	17.6	17.6	N/A	27.4 (6)
	X3LYP	19.5	19.0	19.0	N/A	25.1 (5-trans-syn)
	B3LYP	20.7	20.2	20.2	N/A	25.9 (5-trans-syn)
	M05	3.6	3.1	0.3	-6.4 (10-cis)	5.4 (5-cis-anti)
	B1B95	4.2	3.8	0.2	-8.1 (1)	5.0 (5-cis-syn)
DH	PW6B95	5.8	4.7	3.2	-5.3 (1)	9.9 (6)
	TPSSh	8.0	7.6	7.5	-1.9 (1)	11.0 (5-cis-anti)
	MN15	8.3	6.9	-4.2	-15.2 (10-trans)	7.6 (6)
	M06	8.5	7.1	6.7	-1.7 (1)	16.6 (6)
	BMK	9.0	8.1	-0.4	-16.6 (10-cis)	11.4 (5-trans-syn)
	M08-HX	11.2	8.8	-6.9	-21.8 (10-cis)	8.1 (6)
	M05-2X	11.6	9.7	-5.0	-22.3 (10-cis)	15.7 (6)
DH	M06-2X	15.4	12.3	-11.5	-28.4 (10-cis)	7.7 (6)
	τ -HCTH \hbar	17.1	16.9	16.9	N/A	20.1 (5-cis-anti)
	M06-HF	26.8	22.0	-18.5	-51.9 (10-cis)	15.4 (6)
	wB97X-D	7.0	6.1	1.6	-9.8 (11)	10.7 (6)
	N12-SX	7.3	6.4	6.0	-2.8 (1)	11.6 (5-cis-syn)
	MN12-SX	9.2	7.7	-4.8	-17.8 (10-cis)	12.3 (6)
	M11	9.8	8.7	-1.7	-17.9 (10-trans)	11.6 (6)
DH	ω B97X	10.7	9.0	-4.8	-21.0 (11)	11.1 (6)
	CAM-B3LYP	11.5	9.3	7.9	-5.2 (10-cis)	21.6 (6)
	LC-BLYP	13.8	11.7	-4.3	-26.1 (11)	17.7 (6)
	ω B97	15.2	12.1	-10.6	-29.0 (11)	8.4 (6)
	LC- ω HPBE	16.8	13.7	-13.7	-31.0 (11)	N/A
	LC- ω PBE	16.8	13.7	-13.7	-31.0 (11)	N/A
	LC-BP86	19.4	15.9	-15.8	-35.3 (11)	0.1 (6)
DH	LC-BPW91	21.0	17.9	-17.9	-37.1 (11)	N/A
	LC-PBEPBE	21.8	19.0	-19.0	-37.9 (11)	N/A
	B2GP-PLYP	3.6	3.2	-1.2	-6.1 (1)	6.0 (6)
	B2T-PLYP	3.8	2.9	2.2	-2.8 (1)	8.4 (6)
	DSD-BLYP	5.6	4.8	-4.7	-9.8 (7-trans-syn)	0.9 (6)
	mPW2-PLYP	6.2	5.3	5.3	N/A	11.9 (6)
	B2-PLYP	7.7	7.4	7.4	N/A	10.5 (5-cis-syn)
DH	B2K-PLYP	7.7	6.6	-6.2	-12.5 (7-trans-syn)	3.9 (6)

(Continues)

Table 5. Continued

Type ^[a]	Method	RMSD ^[b]	MAD ^[b]	MSD ^[b]	LND ^{[b],[c]}	LPD ^{[b],[c]}
PBE0-DH		8.7	7.4	-7.2	-15.6 (10-cis)	2.1 (6)
DSD-PBEP86		9.0	8.6	-8.6	-13.5 (7-trans-syn)	N/A
PBEQI-DH		14.7	14.1	-14.1	-20.0 (1)	N/A

[a] Footnote a to Table 2 applies here.
[b] Footnote b to Table 4 applies here.
[c] The reaction with the LND/LPD is given in parenthesis (see Figs. 1 and 2).

Table 6. Average RMSDs (in kJ mol^{-1}) for all functionals from each rung of Jacob's ladder for the barrier heights and reaction energies in the Criegee22 database. The average RMSDs are calculated from the RMSDs listed in Tables 4 and 5.

Type ^[a]	Number of functionals	Barrier heights	Reaction energies
GGA	8	7.6	28.7
MGGA	8	5.4	17.2
HGGA	17	6.6	10.9
HMGGA	12	6.5	10.8
RS	13	7.4	13.9
DH	9	6.7	7.4

[a] Footnote a to Table 2 applies here.

obtained from Kohn–Sham DFT calculations.^[145,146] Let us begin with the performance of the MP2-based procedures for the reaction energies and barrier heights in the Criegee22 database. The performance of these methods is evaluated in conjunction with the Def2-QZVPP basis set to enable a direct comparison with the DHDFT results in Tables 4 and 5. It is clear that none of the MP2-based methods can compete with the performance of the DHDFT methods. The RMSDs for the reaction barrier

heights range between 6.6 (SCSN-MP2) and 15.5 (S2-MP2) kJ mol^{-1} . The RMSDs for the reaction energies are much larger and range between 20.3 (SCSN-MP2) and 31.6 (S2-MP2) kJ mol^{-1} .

The CCSD(T) method in conjunction with nonaugmented double- ζ -quality basis sets performs reasonably well for the reaction barrier heights with RMSDs of 3.4 (6-31G(d)), 2.9 (6-31G(2df,p)), and 3.8 (cc-pVDZ) kJ mol^{-1} ; however, it results in very high RMSDs of over 15 kJ mol^{-1} for the reaction energies. Addition of diffuse functions significantly improves the performance for the reaction energies. In particular, the 6-31+G(d) and aug-cc-pVDZ basis set result in RMSDs of 4.2 and 3.6 kJ mol^{-1} , respectively.

A cost-effective approach for approximating the CCSD(T)/CBS energy is using the following additivity-based scheme: CCSD(T)/CBS(MP2) = CCSD(T)/VDZ + $\Delta\text{MP2/CBS}$. The MP2-based basis-set correction term is taken as: $\Delta\text{MP2/CBS} = \text{MP2}/V\{T,Q\}Z - \text{MP2}/\text{VDZ}$, where the $\text{MP2}/V\{T,Q\}Z$ energy is extrapolated to the basis-set limit with an extrapolation exponent of 3.0.^[147] This additivity scheme has been found to be an efficient way for approximating reaction energies^[144,148,149] and barrier heights^[139,140,144] at the CCSD(T)/CBS level. Using this approach

Table 7. Overview of the performance of a representative set of DFT functionals across the rungs of Jacob's Ladder with and without empirical D3 and D3BJ dispersion corrections. The tabulated values are $\Delta\text{D3} = \text{RMSD(DFT)} - \text{RMSD(DFT-D3)}$ and $\Delta\text{D3BJ} = \text{RMSD(DFT)} - \text{RMSD(DFT-D3BJ)}$ (in kJ mol^{-1}).^[a]

Type ^[b]	Method	Barrier heights		Reaction energies	
		ΔD3	ΔD3BJ	ΔD3	ΔD3BJ
GGA	BLYP	-0.1	0.3	-0.3	-0.9
	PBE	-0.1	0.1	-0.2	-0.4
MGGA	BP86	-0.1	0.2	-0.3	-0.7
	M06-L	0.0	N/A	0.0	N/A
HGGA	TPSS	0.0	0.1	-0.2	-0.6
	B3LYP	-0.2	0.2	-0.2	-0.7
HMGGA	B3PW91	-0.2	0.2	-0.2	-0.7
	PBEO	-0.1	0.1	-0.1	-0.3
HMGGA	PW6B95	-0.1	0.0	0.0	-0.1
	M05	-0.1	N/A	0.0	N/A
HMGGA	M05-2X	0.0	N/A	0.0	N/A
	M06	0.0	N/A	-0.1	N/A
HMGGA	M06-2X	0.0	N/A	0.0	N/A
	M06-HF	0.0	N/A	0.1	N/A
RS	BMK	-0.2	0.1	0.1	0.1
	CAM-B3LYP	-0.1	0.1	-0.1	-0.2
DH	LC-wPBE	-0.1	0.1	0.2	0.4
	B2-PLYP	N/A	0.1	N/A	-0.3
DH	DSD-PBEP86	N/A	0.1	N/A	0.3

[a] A positive value indicates the dispersion correction improves the performance of the functional, whereas a negative value indicates deterioration in performance.

[b] Footnote a to Table 2 applies here.

Table 8. Statistical analysis for the performance of standard and composite ab initio procedures for the reaction energies and barrier heights in the Criegee22 database (in kJ mol^{-1}). The CCSDT(Q)/CBS reference values are given in Table 3.

	Method	Basis set	RMSD ^[a]	MAD ^[a]	MSD ^[a]	LND ^{[a],[b]}	LPD ^{[a],[b]}
Barrier heights	MP2	Def2-QZVPP	15.3	13.2	13.2	N/A	33.4 (10-trans)
	SCS-MP2	Def2-QZVPP	12.7	10.7	10.7	N/A	30.0 (10-trans)
	SOS-MP2	Def2-QZVPP	11.5	9.5	9.5	N/A	28.4 (10-trans)
	SCS(MI)-MP2	Def2-QZVPP	8.5	6.8	6.6	-1.3 (5-cis-anti)	20.9 (10-trans)
	SCSN-MP2	Def2-QZVPP	6.6	5.5	4.5	-4.0 (5-cis-anti)	16.2 (10-trans)
	S2-MP2	Def2-QZVPP	15.5	13.4	13.4	N/A	34.2 (10-trans)
	CCSD(T)	6-31G(d)	3.4	2.5	-1.2	-7.4 (4-cis)	3.8 (7-trans-syn)
	CCSD(T)	6-31 + G(d)	2.9	2.5	-1.9	-6.2 (5-cis-anti)	1.6 (6)
	CCSD(T)	6-31G(2df,p)	2.9	2.4	0.5	-4.7 (6)	5.8 (7-trans-syn)
	CCSD(T)	cc-pVDZ	3.8	2.9	-0.8	-8.2 (3-cis)	6.1 (7-trans-syn)
	CCSD(T)	aug-cc-pVDZ	4.3	4.1	-4.1	-5.8 (3-cis)	N/A
	CCSD(T)	CBS(MP2) ^[c]	1.4	1.0	-0.2	-3.6 (10-trans)	2.3 (4-cis)
	CCSD(T)	CBS(MP2) ^[d]	0.5	0.4	-0.2	-0.9 (7-trans-syn)	0.8 (6)
	G4		0.9	0.7	0.2	-2.5 (5-cis-syn)	1.6 (4-cis)
	G3B3		3.2	1.9	0.7	-1.7 (8-cis)	10.8 (10-trans)
	G4(MP2)		1.5	1.3	1.1	-2.0 (5-cis-syn)	2.4 (4-cis)
	G4(MP2)-6X		1.6	1.4	1.3	-1.7 (5-cis-syn)	2.7 (4-cis)
Reaction energies	G3(MP2)B3		3.6	2.0	1.6	-1.5 (6)	11.7 (10-trans)
	CBS-QB3		0.8	0.7	-0.5	-1.6 (11)	0.7 (10-cis)
	MP2	Def2-QZVPP	30.2	29.8	-29.8	-40.1 (7-trans-syn)	N/A
	SCS-MP2	Def2-QZVPP	30.9	30.3	-30.3	-42.1 (7-trans-syn)	N/A
	SOS-MP2	Def2-QZVPP	31.5	30.5	-30.5	-43.0 (7-trans-syn)	N/A
	SCS(MI)-MP2	Def2-QZVPP	23.1	21.1	-20.9	-34.0 (11)	1.7 (6)
	SCSN-MP2	Def2-QZVPP	20.3	17.4	-16.2	-33.3 (10-trans)	13.2 (6)
	S2-MP2	Def2-QZVPP	31.6	31.2	-31.2	-41.8 (7-trans-syn)	N/A
	CCSD(T)	6-31G(d)	15.9	15.5	-15.5	-24.0 (6)	N/A
	CCSD(T)	6-31 + G(d)	4.2	3.7	-2.9	-7.7 (11)	2.5 (3-trans)
	CCSD(T)	6-31G(2df,p)	16.8	16.5	-16.5	-24.3 (6)	N/A
	CCSD(T)	cc-pVDZ	15.2	14.2	-14.2	-27.8 (6)	N/A
	CCSD(T)	aug-cc-pVDZ	3.6	2.9	-2.6	-7.4 (11)	1.7 (6)
	CCSD(T)	CBS(MP2) ^[c]	1.7	1.4	-1.1	-4.1 (6)	0.8 (2-cis)
	CCSD(T)	CBS(MP2) ^[d]	4.1	3.7	-3.7	-7.9 (11)	N/A
	G4		3.6	3.4	-3.4	-6.8 (5-cis-syn)	N/A
	G3B3		2.5	2.0	-1.9	-6.7 (11)	0.7 (1)
	G4(MP2)		2.9	2.5	-2.5	-6.3 (5-cis-syn)	N/A
	G4(MP2)-6X		3.2	2.8	-2.8	-6.3 (5-cis-syn)	N/A
	G3(MP2)B3		2.2	1.7	-1.4	-5.7 (11)	1.7 (1)
	CBS-QB3		6.3	6.2	-6.2	-8.8 (11)	N/A

[a] Footnote b to Table 4 applies here.

[b] The reaction with the LND/LPD is given in parenthesis (see Figs. 1 and 2).

[c] CCSD(T)/CBS(MP2) = CCSD(T)/cc-pVDZ + MP2/cc-pV(T,Q)Z - MP2/cc-pVDZ.

[d] CCSD(T)/CBS(MP2) = CCSD(T)/aug-cc-pVDZ + MP2/aug-cc-pV(T,Q)Z - MP2/aug-cc-pVDZ.

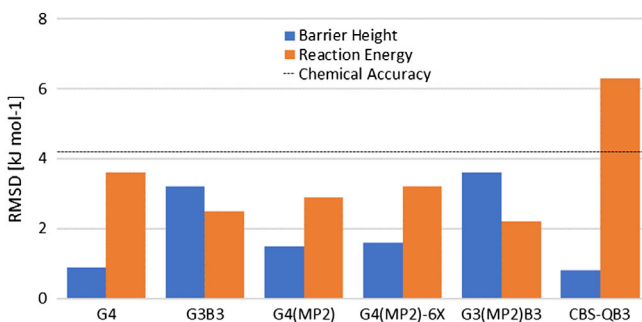


Figure 4. Root-mean-square deviations (RMSDs) of composite ab initio procedures over the barrier heights (shown in blue) and reaction energies (shown in orange) relative to the Criegee22 database (in kJ mol^{-1}). The “chemical accuracy” threshold (dashed black line) represents an RMSD of 4.2 kJ mol^{-1} . The RMSDs of all the composite procedures are given in Table 8. [Color figure can be viewed at wileyonlinelibrary.com]

in conjunction with the regular cc-pVnZ basis sets results in remarkably low RMSDs of 1.4 (for barrier heights) and 1.7 (for reaction energies) kJ mol^{-1} . The use of the aug-cc-pVnZ basis sets results in an RMSD of merely 0.5 kJ mol^{-1} for the barrier heights, however the RMSD for the reaction energies increases to 4.1 kJ mol^{-1} . Thus, it seems that the use of nonaugmented basis sets benefits from a certain degree of error cancelation between basis set incompleteness and the neglection of higher-order correlation for the reaction energies in the Criegee22 database.

Table 8 and Figure 4 give an overview of the performance of the Gaussian-*n* and CBS-QB3 composite methods. The CBS-QB3 procedure shows excellent performance for barrier heights (RMSD = 0.8 kJ mol^{-1}) but relatively poor performance for reaction energies (RMSD = 6.3 kJ mol^{-1}). All the considered Gaussian-*n* methods show good performance with RMSDs well

Table 9. RMSDs for the best performing DFT and ab initio procedures (in kJ mol^{-1}). The CCSDT(Q)/CBS reference values are given in Table 3.

Type	Method	Barrier heights	Reaction energies	Overall ^[a]
Standard ab initio	CCSD(T)/CBS(MP2) ^[b]	1.4	1.7	1.6
	CCSD(T)/CBS(MP2) ^[c]	0.5	4.1	2.3
	CCSD(T)/6-31+G(d)	2.9	4.2	3.5
Composite ab initio	G4(MP2)	1.5	2.9	2.2
	G4	0.9	3.6	2.3
	G4(MP2)-6X	1.6	3.2	2.4
	G3(MP2)B3	3.6	2.2	2.9
	G3B3	3.2	2.5	2.9
	MN12-L	3.5	4.7	4.1

[a] Average of RMSDs for the reaction energies and barrier heights.
[b] CCSD(T)/CBS(MP2) = CCSD(T)/cc-pVDZ + MP2/cc-pV(T,Q)Z – MP2/cc-pVDZ.
[c] CCSD(T)/CBS(MP2) = CCSD(T)/aug-cc-pVDZ + MP2/aug-cc-pV(T,Q)Z – MP2/aug-cc-pVDZ.

below the threshold of chemical accuracy for both reaction energies and barrier heights. For reaction barrier heights G4 emerges as the best method with an RMSD of 0.9 kJ mol^{-1} , for reaction energies G3(MP2)B3 gives the best performance with an RMSD of 2.2 kJ mol^{-1} .

Overall recommendations for both reaction energies and barrier heights

In practical applications of quantum chemical methods, we usually want to use methods that are able to accurately describe all aspects of the potential energy surface (i.e., give both reliable reaction energies and barrier heights). Based on the results of the previous sections, here we identify DFT and standard/composite ab initio methods that give RMSDs $< 5 \text{ kJ mol}^{-1}$ for both reaction energies and barrier heights. These methods are listed in Table 9.

Of the considered standard ab initio methods, the non-empirical CCSD(T)/CBS(MP2) approach in conjunction with the cc-pVnZ basis sets is the most recommended. Importantly, this is the only method that results in RMSDs $< 2 \text{ kJ mol}^{-1}$ for both reaction energies and barrier heights. The G4(MP2) method is a close second, with RMSDs of 2.9 and 1.5 kJ mol^{-1} for reaction energies and barrier heights, respectively. Of the 58 conventional DFT considered, only the meta-GGA MN12-L functional attains RMSDs $< 5 \text{ kJ mol}^{-1}$ for both reaction energies and barrier heights. Therefore, it is the recommended method for investigations involving Cls that are too large for the application of the above recommended ab initio methods.

Conclusions

We introduce a representative benchmark database of 22 barrier heights and reaction energies for ring-closing reactions involving Cls (also known as the Criegee22 database). The reference reaction energies and barrier heights are obtained at the CCSDT(Q)/CBS level by means of the W3lite-F12 composite method. The reference barrier heights spread over a wide range of $28.0\text{--}112.9 \text{ kJ mol}^{-1}$, while the reaction energies (all exothermic) range between 70.5 and $150.3 \text{ kJ mol}^{-1}$. These high-level benchmark values allow us to assess the performance of a variety of contemporary DFT, DHDFT, MP2-based, CCSD(T), and

composite ab initio procedures. We considered a total of 67 DFT methods: eight GGA, eight meta-GGA, 17 hybrid-GGA, 12 hybrid-meta-GGA, 13 range-separated, and nine double-hybrid functionals, as well as 13 standard and 6 composite ab initio methods.

With regard to the performance of the conventional DFT and DHDFT procedures we make the following observations:

- Of all the considered DFT and DHDFT methods, only the meta-GGA MN12-L attains good performance for both reaction barrier heights and reaction energies, with RMSDs of 3.5 and 4.7 kJ mol^{-1} , respectively.
- A fair number of DFT methods attain excellent performance for reaction barrier heights (RMSDs are given in parenthesis): BLYP (3.0), TPSS (2.1), MN12-L (3.5), MN15-L (3.6), MN15 (2.1), TPSSh (2.6), and MN12-SX (3.3 kJ mol^{-1}). Surprisingly, none of the DHDFT methods attain RMSDs $< 5 \text{ kJ mol}^{-1}$.
- Nearly all of the DFT and DHDFT procedures attain poor performance for the reaction energies. The few exceptions are (RMSDs are given in parenthesis): M05 (3.6), B1B95 (4.2), B2GP-PLYP (3.6), and B2T-PLYP (3.8 kJ mol^{-1}).
- Empirical dispersion corrections have a minor effect on performance.

With regard to the performance of standard and ab initio procedures, we draw the following conclusions:

- Overall, the cost-effective CCSD(T)/CBS(MP2) = CCSD(T)/cc-pVDZ + MP2/cc-pV(T,Q)Z – MP2/cc-pVDZ approach attains the best performance for both barrier heights and reaction energies, with RMSDs of 1.4 and 1.7 kJ mol^{-1} , respectively.
- Of the composite procedures, G4(MP2) shows the best overall performance with RMSDs of 1.5 and 2.9 kJ mol^{-1} for barrier heights and reaction energies, respectively.
- All MP2-based procedures show poor performance for both reaction energies and barrier heights.

Acknowledgments

This research was undertaken with the assistance of resources from the National Computational Infrastructure (NCI), which is

supported by the Australian Government. We also acknowledge the system administration support provided by the Faculty of Science at the University of Western Australia to the Linux cluster of the Karton group.

Keywords: Criegee intermediate · density functional theory · ab initio methods · CCSDT(Q) · G4(MP2) theory

How to cite this article: C. D. Smith, A. Karton. *J. Comput. Chem.* **2019**, 9999, 1–12. DOI: 10.1002/jcc.26106

 Additional Supporting Information may be found in the online version of this article.

- [1] R. Criegee, *Angew. Chem. Int. Ed.* **1975**, 14, 745.
- [2] L. Vereecken, D. R. Glowacki, M. J. Pilling, *Chem. Rev.* **2015**, 115, 4063.
- [3] C. A. Taatjes, D. E. Shallcross, C. J. Percivalc, *Phys. Chem. Chem. Phys.* **2014**, 16, 1704.
- [4] L. Vereecken, J. S. Francisco, *Chem. Soc. Rev.* **2012**, 41, 6259.
- [5] G. J. R. Aroeira, A. S. Abbott, S. N. Elliott, J. M. Turney, H. F. Schaefer, *Phys. Chem. Chem. Phys.* **2019**, 21, 17760.
- [6] B. Long, J. L. Bao, D. G. Truhlar, *J. Am. Chem. Soc.* **2016**, 138, 14409.
- [7] M. Kettner, A. Karton, A. J. McKinley, D. A. Wild, *Chem. Phys. Lett.* **2015**, 621, 193.
- [8] H. G. Kjaergaard, T. Kurtén, L. B. Nielsen, S. Jørgensen, P. O. Wennberg, *J. Phys. Chem. Lett.* **2013**, 4, 2525.
- [9] A. Karton, M. Kettner, D. A. Wild, *Chem. Phys. Lett.* **2013**, 585, 15.
- [10] S. E. Wheeler, D. H. Ess, K. N. Houk, *J. Phys. Chem. A* **2008**, 112, 1798.
- [11] D. K. Deb, B. Sarkar, *Phys. Chem. Chem. Phys.* **2019**, 21, 14589.
- [12] R. Chhantyal-Pun, R. J. Shannon, D. P. Tew, R. L. Caravan, M. Duchi, C. Wong, A. Ingham, C. Feldman, M. R. McGillen, M. A. H. Khan, et al., *Phys. Chem. Chem. Phys.* **2019**, 21, 14042.
- [13] B. Long, J. L. Bao, D. G. Truhlar, *Nat. Commun.* **2019**, 10, 2003.
- [14] M. H. Almatarneh, I. A. Elayan, M. Altarawneh, J. W. Hollett, *Theor. Chem. Acc.* **2019**, 138, 30.
- [15] N. A. I. Watson, J. A. Black, T. M. Stonelake, P. J. Knowles, J. M. Beams, *J. Phys. Chem. A* **2019**, 123, 218.
- [16] X. Lei, Y. Liu, W. Wang, W. Wang, *Chem. Phys. Lett.* **2019**, 730, 165.
- [17] X. Lin, Q. Meng, B. Feng, Y. Zhai, Y. Li, Y. Yu, Z. Li, X. Shan, F. Liu, L. Zhang, L. Sheng, *J. Phys. Chem. A* **2019**, 123, 1929.
- [18] F. Sarrami, F. Mackenzie-Rae, A. Karton, *Int. J. Quantum Chem.* **2018**, 118, e25599.
- [19] V. P. Barber, S. Pandit, A. M. Green, N. Trongsiriyat, P. J. Walsh, S. J. Klippenstein, M. I. Lester, *J. Am. Chem. Soc.* **2018**, 140, 10866.
- [20] P. Deng, L. Wang, L. Wang, *J. Phys. Chem. A* **2018**, 122, 3013.
- [21] T. Banu, K. Sen, A. K. Das, *J. Phys. Chem. A* **2018**, 122, 8377.
- [22] T. Berndt, H. Herrmann, T. Kurtén, *J. Am. Chem. Soc.* **2017**, 139, 13387.
- [23] G. T. Drozd, T. Kurtén, N. M. Donahue, M. I. Lester, *J. Phys. Chem. A* **2017**, 121, 6036.
- [24] F. Mackenzie-Rae, A. Karton, S. Saunders, *Phys. Chem. Chem. Phys.* **2016**, 18, 27991.
- [25] T. Kurtén, M. P. Rissanen, K. Mackeprang, J. A. Thornton, N. Hyttinen, S. Jørgensen, M. Ehn, H. G. Kjaergaard, *J. Phys. Chem. A* **2015**, 119, 11366.
- [26] L. Jiang, R. Lan, Y. S. Xu, W. J. Zhang, W. Yang, *Int. J. Mol. Sci.* **2013**, 14, 5784.
- [27] T. Kurtén, J. R. Lane, S. Jørgensen, H. G. Kjaergaard, *J. Phys. Chem. A* **2011**, 115, 8669.
- [28] L. Jiang, Y. S. Xu, A. Z. Ding, *J. Phys. Chem. A* **2010**, 114, 12452.
- [29] X. Wang, J. Sun, L. Bao, Q. Mei, B. Wei, Z. An, J. Xie, M. He, *J. Phys. Chem. A* **2019**, 123, 2745.
- [30] I. A. Elayan, M. H. Almatarneh, J. W. Hollett, *Struct. Chem.* **2019**, 30, 1353.
- [31] L. L. B. Bracco, M. E. Tucceri, A. Escalona, Y. Díaz-de-Mara, A. Aranda, A. M. Rodríguez, D. Rodríguez, *Phys. Chem. Chem. Phys.* **2019**, 21, 11214.
- [32] C. Giorio, S. J. Campbell, M. Bruschi, A. T. Archibald, M. Kalberer, *Faraday Discuss.* **2017**, 200, 559.
- [33] C. Giorio, S. J. Campbell, M. Bruschi, F. Tampieri, A. Barbon, A. Toffoletti, A. Tapparo, C. Pajens, A. J. Wedlake, P. Grice, D. J. Howe, M. Kalberer, *J. Am. Chem. Soc.* **2017**, 139, 3999.
- [34] M. H. Almatarneh, E. Al-Shamaileh, Z. M. Ahmad, A. A. -A. Abu-Saleh, I. A. A. Elayan, *Acta Phys. Pol. A* **2017**, 132, 1149.
- [35] H. Wang, R. Zhou, M. Jiang, Z. Lin, Y. Deng, *Comput. Theor. Chem.* **2016**, 1090, 88.
- [36] J. Sun, H. Cao, S. Zhang, X. Li, M. He, *RSC Adv.* **2016**, 6, 113561.
- [37] J. Dang, X. Shi, Q. Zhang, J. Hu, W. Wang, *Sci. Total Environ.* **2015**, 514, 344.
- [38] R. W. Kugel, B. S. Ault, *J. Phys. Chem. A* **2015**, 119, 312.
- [39] B. Schweitzer-Chaput, T. Kurtén, M. Klussmann, *Angew. Chem. Int. Ed.* **2015**, 54, 11848.
- [40] L. Pileno, A. D. Gudmundsdottir, B. S. Ault, *J. Phys. Chem. A* **2013**, 117, 4174.
- [41] T. L. Nguyen, R. Winterhalter, G. Moortgat, B. Kanawati, J. Peeters, L. Vereecken, *Phys. Chem. Chem. Phys.* **2009**, 11, 4173.
- [42] B. Bonn, A. Hirsikko, H. Hakola, T. Kurtén, L. Laasko, M. Boy, M. Dal Maso, J. M. Mäkelä, M. Kulmala, *Atmos. Chem. Phys.* **2007**, 7, 2893.
- [43] T. Kurtén, B. Bonn, H. Vehkämäki, M. Kulmala, *J. Phys. Chem. A* **2007**, 111, 3394.
- [44] A. Karton, J. M. L. Martin, *J. Chem. Phys.* **2012**, 136, 124114.
- [45] A. Karton, I. Kaminker, J. M. L. Martin, *J. Phys. Chem. A* **2009**, 113, 7610.
- [46] A. Karton, *WIREs Comput. Mol. Sci.* **2016**, 6, 292.
- [47] J. P. Perdew, K. Schmidt, *AIP Conf. Proc.* **2000**, 577, 1.
- [48] K. A. Peterson, T. B. Adler, H.-J. Werner, *J. Chem. Phys.* **2008**, 128, 084102.
- [49] J. Noga, S. Kedžuch, J. Šimunek, *J. Chem. Phys.* **2007**, 127, 034106.
- [50] G. Knizia, H.-J. Werner, *J. Chem. Phys.* **2008**, 128, 154103.
- [51] T. B. Adler, G. Knizia, H.-J. Werner, *J. Chem. Phys.* **2007**, 127, 221106.
- [52] K. A. Peterson, T. H. Dunning, *J. Chem. Phys.* **2002**, 117, 10548.
- [53] P. R. Spackman, D. Jayatilaka, A. Karton, *J. Chem. Phys.* **2016**, 145, 104101.
- [54] F. Weigend, R. Ahlrichs, *Phys. Chem. Chem. Phys.* **2005**, 7, 3297.
- [55] L. Goerigk, S. Grimme, *WIREs Comput. Mol. Sci.* **2014**, 4, 576.
- [56] S. Kozuch, J. M. L. Martin, *J. Comput. Chem.* **2013**, 34, 2327.
- [57] S. Kozuch, J. M. L. Martin, *Phys. Chem. Chem. Phys.* **2011**, 13, 20104.
- [58] H. Kruse, J. Sponer, *Int. J. Quantum Chem.* **2018**, 118, e25624.
- [59] S. Grimme, *WIREs Comput. Mol. Sci.* **2011**, 1, 211.
- [60] S. Grimme, J. Antony, S. Ehrlich, H. Krieg, *J. Chem. Phys.* **2010**, 132, 154104.
- [61] S. Grimme, S. Ehrlich, L. Goerigk, *J. Comput. Chem.* **2011**, 32, 1456.
- [62] A. D. Becke, E. R. Johnson, *J. Chem. Phys.* **2005**, 123, 154101.
- [63] C. Lee, W. Yang, R. G. Parr, *Phys. Rev. B* **1988**, 37, 785.
- [64] A. D. Becke, *Phys. Rev. A* **1988**, 38, 3098.
- [65] S. Grimme, *J. Comput.* **1787–1799**, 2006, 27.
- [66] A. D. Boese, N. C. Handy, *J. Chem. Phys.* **2001**, 114, 5497.
- [67] J. P. Perdew, K. Burke, M. Ernzerhof, *Phys. Rev. Lett.* **1996**, 77, 3865.
- [68] J. P. Perdew, *Phys. Rev. B* **1986**, 33, 8822.
- [69] J. P. Perdew, J. A. Chevry, S. H. Vosko, K. A. Jackson, M. R. Pederson, D. J. Singh, C. Fiolhais, *Phys. Rev. B* **1992**, 46, 6671.
- [70] R. Peverati, Y. Zhao, D. G. Truhlar, *J. Phys. Chem. Lett.* **2011**, 2, 1991.
- [71] R. Peverati, D. G. Truhlar, *J. Chem. Theory Comput.* **2012**, 8, 2310.
- [72] Y. Zhao, D. G. Truhlar, *J. Chem. Phys.* **2006**, 125, 194101.
- [73] J. M. Tao, J. P. Perdew, V. N. Staroverov, G. E. Scuseria, *Phys. Rev. Lett.* **2003**, 91, 146401.
- [74] A. D. Boese, N. C. Handy, *J. Chem. Phys.* **2002**, 116, 9559.
- [75] T. van Voorhis, G. E. Scuseria, *J. Chem. Phys.* **1998**, 109, 400.
- [76] A. D. Becke, *J. Chem. Phys.* **1996**, 104, 1040.
- [77] R. Peverati, D. G. Truhlar, *J. Phys. Chem. Lett.* **2012**, 3, 117.
- [78] R. Peverati, D. G. Truhlar, *Phys. Chem. Chem. Phys.* **2012**, 10, 13171.
- [79] H. S. Yu, X. He, S. L. Li, D. G. Truhlar, *Chem. Sci.* **2016**, 7, 5032.
- [80] A. D. Becke, *J. Chem. Phys.* **1993**, 98, 1372.
- [81] A. D. Becke, *J. Chem. Phys.* **1993**, 98, 5648.
- [82] P. J. Stephens, F. J. Devlin, C. F. Chabalowski, M. J. Frisch, *J. Phys. Chem.* **1994**, 98, 11623.
- [83] C. Adamo, V. Barone, *J. Chem. Phys.* **1999**, 110, 6158.
- [84] F. A. Hamprecht, A. J. Cohen, D. J. Tozer, N. C. Handy, *J. Chem. Phys.* **1998**, 109, 6264.

- [85] H. L. Schmider, A. D. Becke, *J. Chem. Phys.* **1998**, *108*, 9624.
- [86] X. Xu, Q. Zhang, R. P. Muller, W. A. Goddard, *J. Chem. Phys.* **2005**, *122*, 014105.
- [87] R. Peverati, D. G. Truhlar, *J. Chem. Phys.* **2011**, *135*, 191102.
- [88] A. Austin, G. Petersson, M. J. Frisch, F. J. Dobek, G. Scalmani, K. Throssell, *J. Chem. Theory Comput.* **2012**, *8*, 4989.
- [89] C. Adamo, V. Barone, *J. Chem. Phys.* **1998**, *108*, 664.
- [90] J. Heyd, G. E. Scuseria, M. Ernzerhof, *J. Chem. Phys.* **2003**, *118*, 8207.
- [91] A. V. Kruckau, O. A. Vydrov, A. F. Izmaylov, G. E. Scuseria, *J. Chem. Phys.* **2006**, *125*, 224106.
- [92] Y. Zhao, N. E. Schultz, D. G. Truhlar, *J. Chem. Phys.* **2005**, *123*, 161103.
- [93] Y. Zhao, N. E. Schultz, D. G. Truhlar, *J. Chem. Theory Comput.* **2006**, *2*, 364.
- [94] Y. Zhao, D. G. Truhlar, *Theor. Chem. Acc.* **2008**, *120*, 215.
- [95] Y. Zhao, D. G. Truhlar, *J. Chem. Theory Comput.* **2008**, *4*, 1849.
- [96] A. D. Boese, J. M. L. Martin, *J. Chem. Phys.* **2004**, *121*, 3405.
- [97] V. N. Staroverov, G. E. Scuseria, J. Tao, J. P. Perdew, *J. Chem. Phys.* **2003**, *119*, 12129.
- [98] Y. Zhao, D. G. Truhlar, *J. Phys. Chem. A* **2005**, *109*, 5656.
- [99] J.-D. Chai, M. Head-Gordon, *J. Chem. Phys.* **2008**, *084106*, 128.
- [100] J.-D. Chai, M. Head-Gordon, *Phys. Chem. Chem. Phys.* **2008**, *10*, 6615.
- [101] R. Peverati, D. G. Truhlar, *J. Phys. Chem. Lett.* **2011**, *2*, 2810.
- [102] R. Peverati, D. G. Truhlar, *Phys. Chem. Chem. Phys.* **2012**, *14*, 16187.
- [103] T. Yanai, D. Tew, N. Handy, *Chem. Phys. Lett.* **2004**, *393*, 51.
- [104] T. M. Henderson, A. F. Izmaylov, G. Scalmani, G. E. Scuseria, *J. Chem. Phys.* **2009**, *131*, 044108.
- [105] O. A. Vydrov, G. E. Scuseria, *J. Chem. Phys.* **2006**, *125*, 234109.
- [106] H. Iikura, T. Tsuneda, T. Yanai, K. Hirao, *J. Chem. Phys.* **2001**, *115*, 3540.
- [107] S. Grimme, *J. Chem. Phys.* **2006**, *124*, 034108.
- [108] T. Schwabe, S. Grimme, *Phys. Chem. Chem. Phys.* **2006**, *8*, 4398.
- [109] É. Brémond, C. Adamo, *J. Chem. Phys.* **2011**, *135*, 024106.
- [110] É. Brémond, J. C. Sancho-García, Á. J. Pérez-Jiménez, C. Adamo, *J. Chem. Phys.* **2014**, *141*, 031101.
- [111] A. Karton, A. Tarnopolsky, J.-F. Lamere, G. C. Schatz, J. M. L. Martin, *J. Phys. Chem. A* **2008**, *112*, 12868.
- [112] A. Tarnopolsky, A. Karton, R. Sertchook, D. Vuzman, J. M. L. Martin, *J. Phys. Chem. A* **2008**, *112*, 3.
- [113] S. Kozuch, D. Gruzman, J. M. L. Martin, *J. Phys. Chem. C* **2010**, *114*, 20801.
- [114] S. Grimme, *J. Chem. Phys.* **2003**, *118*, 9095.
- [115] Y. Jung, R. C. Lochan, A. D. Dutoi, M. Head-Gordon, *J. Chem. Phys.* **2004**, *121*, 9793.
- [116] R. A. Distasio, M. Head-Gordon, *Mol. Phys.* **2007**, *105*, 1073.
- [117] J. G. Hill, J. A. Platts, *J. Chem. Theory Comput.* **2007**, *3*, 80.
- [118] R. F. Fink, *J. Chem. Phys.* **2010**, *133*, 174113.
- [119] K. Raghavachari, G. W. Trucks, J. A. Pople, M. Head-Gordon, *Chem. Phys. Lett.* **1989**, *157*, 479.
- [120] R. J. Bartlett, M. Musial, *Rev. Mod. Phys.* **2007**, *79*, 291.
- [121] L. A. Curtiss, P. C. Redfern, K. Raghavachari, *J. Chem. Phys.* **2007**, *126*, 084108.
- [122] L. A. Curtiss, P. C. Redfern, K. Raghavachari, *J. Chem. Phys.* **2007**, *127*, 124105.
- [123] B. Chan, J. Deng, L. Radom, *J. Chem. Theory Comput.* **2011**, *7*, 112.
- [124] A. G. Baboul, L. A. Curtiss, P. C. Redfern, K. Raghavachari, *J. Chem. Phys.* **1999**, *110*, 7650.
- [125] J. A. Montgomery, Jr., M. J. Frisch, J. W. Ochterski, G. A. Petersson, *J. Chem. Phys.* **1999**, *110*, 2822.
- [126] Werner, H.-J., Knowles, P. J., Knizia, G., Manby, F. R., Schutz, M., Celani, P., Korona, T., Lindh, R., Mitrushenkov, A., Rauhut, G., et al. MOLPRO (version 2012.1) is a package of ab initio programs. Available at: <http://www.molpro.net>.
- [127] H.-J. Werner, P. J. Knowles, G. Knizia, F. R. Manby, M. Schutz, *WIREs Comput. Mol. Sci.* **2012**, *2*, 242.
- [128] MRCC, a quantum chemical program suite written by Kállay, M., Nagy, P. R., Rolik, Z., Mester, D., Samu, G., Csontos, J., Csóka, J., Szabó, B. P., Gyevi-Nagy, L., Ladjánszki, I., et al. Available at: <http://www.mrcc.hu>.
- [129] Z. Rolik, L. Szegedy, I. Ladjánszki, B. Ladoczki, M. Kállay, *J. Chem. Phys.* **2013**, *139*, 094105.
- [130] M. J. Frisch, G. W. Trucks, H. B. Schlegel, G. E. Scuseria, M. A. Robb, J. R. Cheeseman, G. Scalmani, V. Barone, G. A. Petersson, H. Nakatsuji, X. Li, M. Caricato, A. V. Marenich, J. Bloino, B. G. Janesko, R. Gomperts, B. Mennucci, H. P. Hratchian, J. V. Ortiz, A. F. Izmaylov, J. L. Sonnenberg, D. Williams-Young, F. Ding, F. Lipparini, F. Egidi, J. Goings, B. Peng, A. Petrone, T. Henderson, D. Ranasinghe, V. G. Zakrzewski, J. Gao, N. Rega, G. Zheng, W. Liang, M. Hada, M. Ehara, K. Toyota, R. Fukuda, J. Hasegawa, M. Ishida, T. Nakajima, Y. Honda, O. Kitao, H. Nakai, T. Vreven, K. Throssell, J. A. Montgomery, Jr., J. E. Peralta, F. Ogliaro, M. J. Bearpark, J. J. Heyd, E. N. Brothers, K. N. Kudin, V. N. Staroverov, T. A. Keith, R. Kobayashi, J. Normand, K. Raghavachari, A. P. Rendell, J. C. Burant, S. S. Iyengar, J. Tomasi, M. Cossi, J. M. Millam, M. Klene, C. Adamo, R. Cammi, J. W. Ochterski, R. L. Martin, K. Morokuma, O. Farkas, J. B. Foresman, D. J. Fox, Gaussian 16, Revision A.03, Gaussian, Inc., Wallingford, CT, **2016**.
- [131] A. Karton, *J. Phys. Chem. A* **2019**, *123*, 6720.
- [132] J. M. L. Martin, G. de Oliveira, *J. Chem. Phys.* **1999**, *111*, 1843.
- [133] D. Stone, K. Au, S. Sime, D. J. Medeiros, M. Blitz, P. W. Seakins, Z. Decker, L. Sheps, *Phys. Chem. Chem. Phys.* **2018**, *20*, 24940.
- [134] L. Goerigk, S. Grimme, *J. Chem. Theory Comput.* **2011**, *7*, 291.
- [135] L. Goerigk, A. Hansen, C. A. Bauer, S. Ehrlich, A. Najibi, S. Grimme, *Phys. Chem. Chem. Phys.* **2017**, *19*, 32184.
- [136] N. Mardirossian, M. Head-Gordon, *Mol. Phys.* **2017**, *115*, 2315.
- [137] J. Zheng, Y. Zhao, D. G. Truhlar, *J. Chem. Theory Comput.* **2009**, *5*, 808.
- [138] A. Karton, R. J. O'Reilly, L. Radom, *J. Phys. Chem. A* **2012**, *116*, 4211.
- [139] A. Karton, L. Goerigk, *J. Comput. Chem.* **2015**, *36*, 622.
- [140] L.-J. Yu, F. Sarrami, R. J. O'Reilly, A. Karton, *Chem. Phys.* **2015**, *458*, 1.
- [141] A. D. Becke, *J. Chem. Phys.* **1997**, *107*, 8554.
- [142] A. Karton, S. Parthiban, J. M. L. Martin, *J. Phys. Chem. A* **2009**, *113*, 4802.
- [143] A. Karton, J. M. L. Martin, *Mol. Phys.* **2012**, *110*, 2477.
- [144] L.-J. Yu, F. Sarrami, R. J. O'Reilly, A. Karton, *Mol. Phys.* **2016**, *114*, 21.
- [145] A. J. C. Varandas, *Phys. Chem. Chem. Phys.* **2018**, *20*, 22084.
- [146] A. J. C. Varandas, *Phys. Chem. Chem. Phys.* **2019**, *21*, 8022.
- [147] A. Halkier, T. Helgaker, P. Jørgensen, W. Klopper, H. Koch, J. Olsen, A. K. Wilson, *Chem. Phys. Lett.* **1998**, *286*, 243.
- [148] L.-J. Yu, A. Karton, *Chem. Phys.* **2014**, *441*, 166.
- [149] J. Friedrich, *J. Chem. Theory Comput.* **2015**, *11*, 3596.

Received: 14 September 2019

Revised: 21 October 2019

Accepted: 22 October 2019